A MicroPirani Pressure Sensor Based on the Tungsten Microhotplate in a Standard CMOS Process

Jiaqi Wang, Zhenan Tang, *Member, IEEE*, Jinfeng Li, and Fengtian Zhang

***Abstract*—This paper reports a tungsten microhotplate fabricated in a standard CMOS process and the implementation of a MicroPirani pressure sensor with it. A monolithic constant-current circuit including an operational amplifier is used to bias the tungsten microhotplate to measure the gas pressure. The sensor shows a linear response to the gas pressure in the range of 1–100 Pa when driven by a constant current of 7 mA. In this regime, the sensitivity of the sensor is 0.23 mV/Pa, the linearity is 4.95%, and the hysteresis is 8.69%. The MicroPirani pressure sensor in this paper can be used in a medium-vacuum measurement. Because tungsten in a standard CMOS process has a large temperature coefficient regardless of the different manufacturing processes, the design of the tungsten microhotplate can be applied to other thermal-based sensors, even in different standard CMOS processes.**

***Index Terms*—CMOS pressure sensor, microelectromechanical systems (MEMS), pressure sensor, tungsten microhotplate.**

I. Introduction

THE DEVELOPMENT of micromachining technology has led to various microelectromechanical systems (MEMS) devices, such as the optical attenuator [1] and the pressure sensor [2]. The Pirani pressure sensor is a thermal-conductivity-type vacuum sensor. Its operation principle is based on the fact that the heat loss of a hotplate to its ambient through gas conduction is proportional to the molecular density of gas in a vacuum system [3]. Many MicroPirani pressure sensors have emerged based on MEMS technology [4]–[7]. They are widely used in vacuum testing, such as in micro vapor-jet pump [8] and MEMS vacuum package [9]. These MicroPirani pressure sensors can provide not only a wider measurement range but also a better sensitivity with lower power consumption. The manufacturing yields of these sensors are also excellent [10]. CMOS-compatible MicroPirani pressure sensors usually employ a surface-micromachined polysilicon microhotplate as the sensing component [11], [12]. In a standard CMOS process, a sandwich structure is fabricated to form the polysilicon microhotplate. The lower polysilicon layer is etched as a sacrificial layer to form the suspended gap. The upper polysilicon layer is used as the heating and the temperature measurement resistor for the microhotplate.

The thickness, resistivity, and temperature coefficient of the polysilicon may vary in different CMOS processes, thus largely affecting the microhotplate design. For instance, the different temperature coefficients of the polysilicon have an effect on the measurement precision of the temperature. More importantly, with the developing manufacturing technology of the integrated circuits, the polysilicon will have a smaller temperature coefficient to meet the demands of the integrated circuit technology. However, the measurement precision of the temperature for the polysilicon microhotplate is greatly limited by a small temperature coefficient. The worst situation is that the polysilicon may be unsuitable for the design of the microhotplate if more advanced manufacturing technologies are adopted, thus greatly limiting the development of CMOS-compatible MicroPirani pressure sensors.

Therefore, it is necessary to design MicroPirani pressure sensors that can be compatible with any standard CMOS process. Paul *et al.* presented a MicroPirani pressure sensor with a microhotplate whose heating resistor was a meander-shaped aluminum thin film [13], [14]. However, aluminum is prone to suffer from a reliability problem known as electromigration. Furthermore, the melting point of aluminum is low. Puers *et al.* described a NanoPirani pressure sensor employing a tungsten microbridge which needed some more complicated manufacturing processes [15]. This paper presents a MicroPirani pressure sensor based on the tungsten microhotplate fabricated in a standard CMOS process. Tungsten (including the barrier metals, such as titanium and titanium nitride) is usually used as the plug material in a standard CMOS process. It is not only resistant to electromigration failure but also has a high melting point. A monolithic constant-current circuit including an operational amplifier is used to bias the tungsten microhotplate to measure the gas pressure. The measurement results show that the sensor based on the tungsten microhotplate has a good response to the gas pressure, particularly from 1 to 100 Pa.

The basic principle of the MicroPirani pressure sensor is introduced in Section II. Section III addresses the fabrication and the characterization of the tungsten microhotplate. The measurement results of the MicroPirani pressure sensor are presented in Section IV, and Section V concludes this paper.

II. Basic Principle of MicroPirani Pressure Sensor Based on the Microhotplate

A schematic drawing of the MicroPirani pressure sensor based on the microhotplate is shown in Fig. 1. Its working

Manuscript received April 18, 2008; revised June 23, 2008 and October 20, 2008. First published January 19, 2009; current version published April 1, 2009. This work was supported by the National Natural Science Foundation of China under Grant 90607003.

J. Wang and J. Li are with the Department of Electronic Engineering, Dalian University of Technology, Dalian 116024, China (e-mail: wjq5003@gmail.com).

Z. Tang is with the Microelectronic Institute, Dalian University of Technology, Dalian 116024, China.

F. Zhang was with the Department of Electronic Engineering, Dalian University of Technology, Dalian 116024, China. He is now with the China Academy of Engineering Physics, Mianyang 621900, China.

Digital Object Identifier 10.1109/TIE.2009.2012421

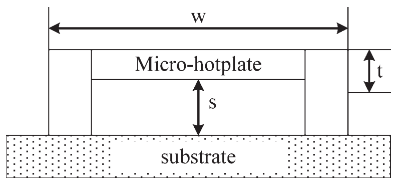

Fig. 1. Schematic drawing of the MicroPirani gas pressure sensor.

principle is based on the fact that the heat loss of a hotplate to its substrate through gas conduction is a function of gas thermal conductivity. Depending on the Knudsen number ($Kn = l/d$, where l is the mean free path of a gas and d is the characteristic dimension of the domain), the regimes of the gas are generally classified as continuum ($Kn < 10^{-2}$), slip flow and temperature jump ($10^{-2} < Kn < 10^{-1}$), or transitional ($10^{-1} < Kn < 1$) and molecular ($Kn > 1$). In each of these regimes, the gas thermal conductivity has different dependence on the gas pressure [16] and characteristic distance. The gas thermal conductivity for the microhotplate can be calculated as [17], [18]

$$k_{\text{gas}}(p) = k_{\text{gas}}(\infty)\left(\frac{p}{p+p_0}\right) \tag{1}$$

$$k_{\text{gas}}(\infty) = k_{\text{gas}}(1\,\text{atm})\left(\frac{p_0+(1\,\text{atm})}{(1\,\text{atm})}\right) \tag{2}$$

$$k_{\text{gas}}(1\,\text{atm}) = \beta\Lambda_0\sqrt{\frac{273.2}{T}} \times P\left(\frac{P_t}{P+P_t}\right) \times s \tag{3}$$

$$p_0 = \frac{1}{2s\left(1+\frac{t}{w}\right)} \tag{4}$$

$$P_t = \frac{9\gamma-5}{\gamma+1}\frac{\lambda_{\text{ref}}}{\beta s} \tag{5}$$

where $k_{\text{gas}}(1\,\text{atm})$ represents the gas thermal conductivity at 1 atm, $k_{\text{gas}}(\infty)$ is the continuum limit, w and t are the width and thickness of the heater, respectively, s is the height of the suspended gap, λ_{ref} is the mean free path of the gas at 1 Pa with the value of 8.11×10^{-3} m, T is the average temperature of the gas, and γ is the ratio of specific heat of gas at constant pressure to specific heat at constant volume with the value of 1.4. The value of β is 0.818, and that of Λ_0 is 1.16 $\text{W}/(\text{m}^2 \cdot \text{KPa})$. Fig. 2 shows the relations between the gas thermal conductivity and the suspended gap under different gas pressures, according to (1)–(5). The gas thermal conductivity relates to the gas pressure, while it also strongly depends on the suspended gap and has a microscale effect. The shorter the height of the suspended gap is, the smaller the gas thermal conductivity is.

The pressure-dependent heat conduction to the substrate combined with the resistive self-heating leads to a pressure-dependent temperature profile in the microhotplate. This can be quantified by measuring the electrical resistance of the microhotplate, since the material's resistivity is temperature dependent [15]. In a typical application, the microhotplate is electrically heated with a bias current that generates an electrical signal representative of the absolute gas pressure [11].

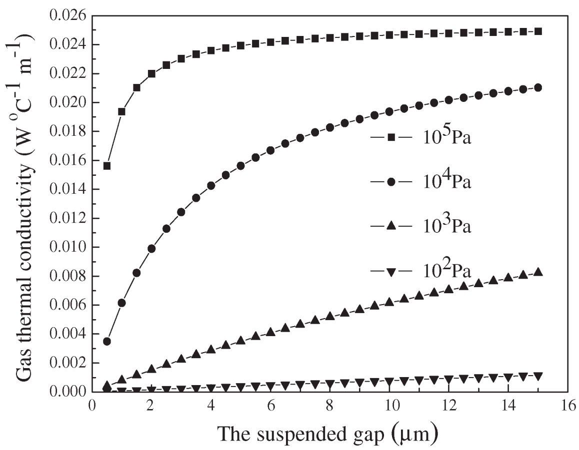

Fig. 2. Relations between the gas thermal conductivity and the suspended gap under different gas pressures.

III. Fabrication and Characteristics of Tungsten Microhotplate

Tungsten has been traditionally used as a plug material to form via pathways between various metal layers and the silicon substrate because of its ability to uniformly fill the high-aspect-ratio vias when deposited by chemical vapor deposition methods. Tungsten is resistant to electromigration failure. It also serves as a barrier to inhibit diffusion and reaction between silicon and the first metal layer [19].

In our design, the tungsten microhotplate is implemented in 0.5-μm CMOS process that features two polysilicon layers (Poly1 and Poly2) and three metal layers (Metal1, Metal2, and Metal3). The metal plug between Metal1 and Metal2 is tungsten, and the one between Metal2 and Metal3 is aluminum. In the design of the tungsten microhotplate, tungsten is employed as the heater in the form of serpentine resistor instead of via plug. The anchors of the tungsten resistor are connected to Metal2, leaving Metal1 unconnected. A 0.34-μm-thick Poly2 is used as a sacrificial layer below the tungsten microhotplate [20]. The etch windows of the tungsten microhotplate are opened during bonding-pad patterning in a standard CMOS process, as shown in Fig. 3(a).

Fig. 3(b) shows that the etch windows and the bonding pads are etched simultaneously during the bonding-pad etching process and that Poly2 is exposed. At last, in Fig. 3(c), Poly2 is removed to suspend the tungsten microhotplate by an improved TMAH etching method which does not etch the exposed aluminum pads [21]. Before starting the process, the new aluminum layer is sputtered at the backside of the die to prevent etching from the backside. About 8 h is required to remove the sacrificial layer in TMAH. Fig. 4(a) and (b) shows the microscope and SEM photographs of the tungsten microhotplate, respectively. The tungsten microhotplate with a square area of 40 μm $\times$ 40 μm is suspended by four beams which have a length of 30 μm and a width of 15 μm. The width of the tungsten resistor is 0.8 μm. The suspended gap between the tungsten microhotplate and the substrate is 0.34 μm.

Fig. 4(c) and (d) shows three tungsten resistors fabricated with different dimensions to test the sheet resistance of tungsten. The ratios of length to width (L/W) of these resistors

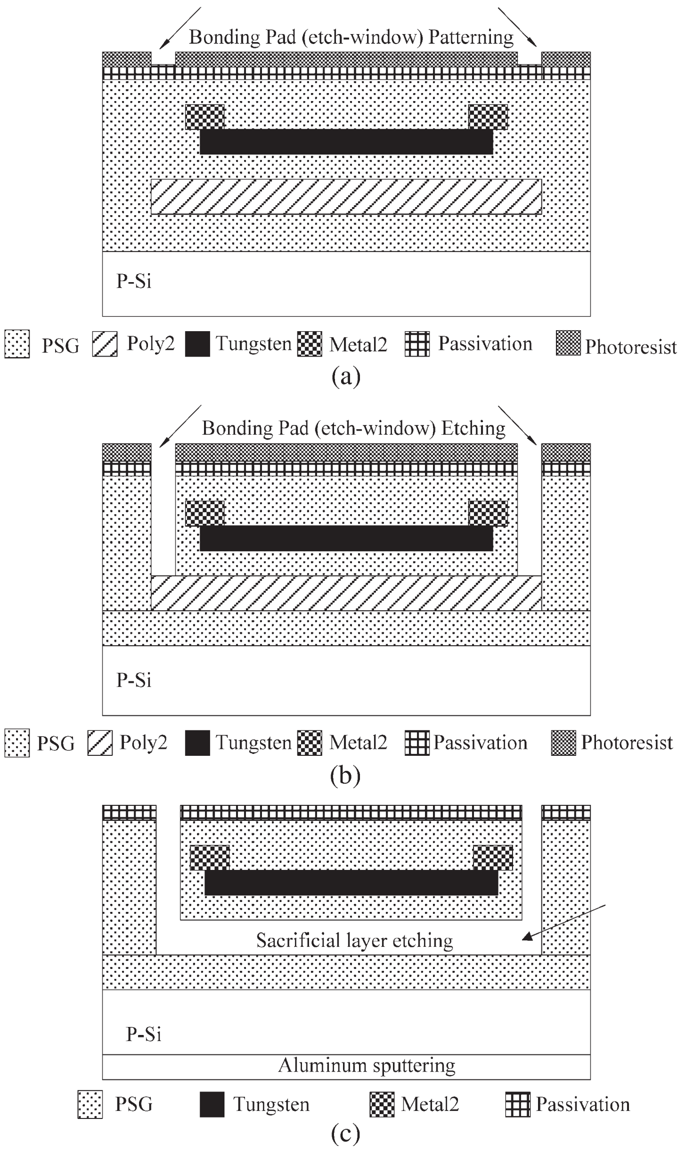

Fig. 3. Schematic of cross sections for the tungsten microhotplate fabrication processes. (a) Tungsten resistor implemented and etch-window opening. (b) Etch-window etching. (c) Tungsten microhotplate suspending.

are 400 μm/2 μm, 200 μm/5 μm, and 100 μm/10 μm, respectively. There are six dies that we have measured. The results are shown in Fig. 5. The sheet resistance of tungsten in the manufacturing process is also estimated to be 0.15 $\Omega/\square$ for a tungsten via plug whose L/W is 1 μm/0.5 μm, and its resistance is 0.3 Ω. With the same dimension, the sheet resistance of tungsten is uniform. However, considering the different dimensions, the sheet resistances could significantly change. The narrower the resistor is, the smaller the sheet resistance is. The reasons may lie in two factors. First, the tungsten layer is a composite one consisting of tungsten, titanium, and titanium nitride which all affect the sheet resistance. Second, the width deviation of each resistor should be considered, particularly for the narrow ones which would have relatively large width deviations.

Tungsten resistors have been encapsulated in the standard IC package and exposed to temperatures ranging from 35 °C to 150 °C. Resistance and temperature are recorded every 5 °C.

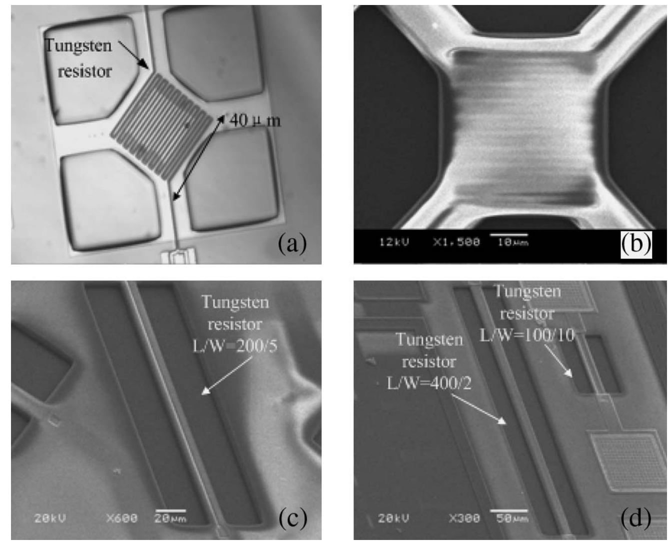

Fig. 4. Fabricated microstructures. (a) Microscope photograph of a tungsten microhotplate. (b) SEM photograph of a tungsten microhotplate. (c) Tungsten resistor with an L/W of 200 μm/5 μm. (d) Tungsten resistors with L/W's of 400 μm/2 μm and 100 μm/10 μm, respectively.

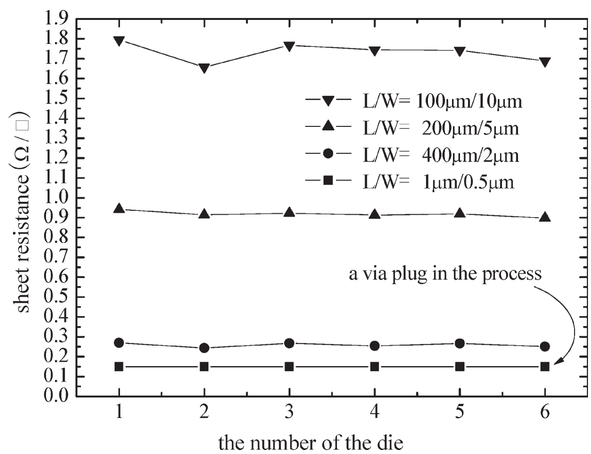

Fig. 5. Sheet resistance of tungsten resistors.

The results are shown in Fig. 6. The temperature coefficient of tungsten is about $1.5 \times 10^{-3}/°\mathrm{C}$.

A current source (Keithley 2400) provides a constant current to the resistor of the tungsten microhotplate, and the voltage drop across the resistor is measured. Temperature is determined from the measured resistance with the temperature coefficient of the resistance. Heating power can be calculated from the current and voltage measured. Then, a linear curve fit is applied to the power versus temperature data to extract thermal impedance that is the slope of the linear curve [17], as shown in Fig. 7. The value of the thermal impedance of the tungsten microhotplate is about 17 $°\mathrm{C/mW}$.

IV. Measurement of the MicroPirani Pressure Sensor

The MicroPirani pressure sensor is driven by a constant-current circuit, which has a good response to the low gas pressure. Due to the large temperature coefficient of tungsten,

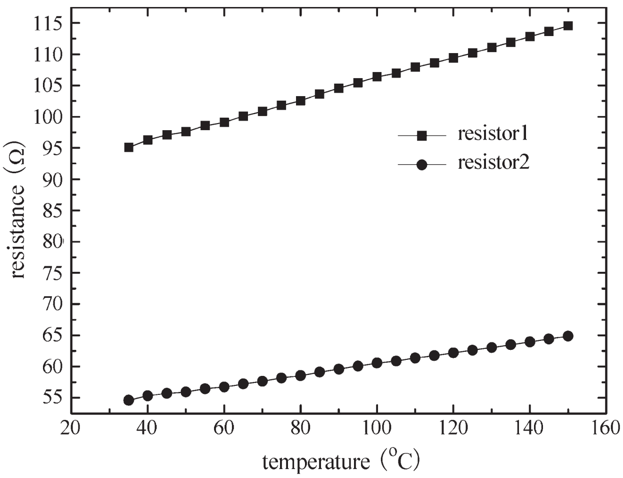

Fig. 6. Temperature coefficient of tungsten resistors.

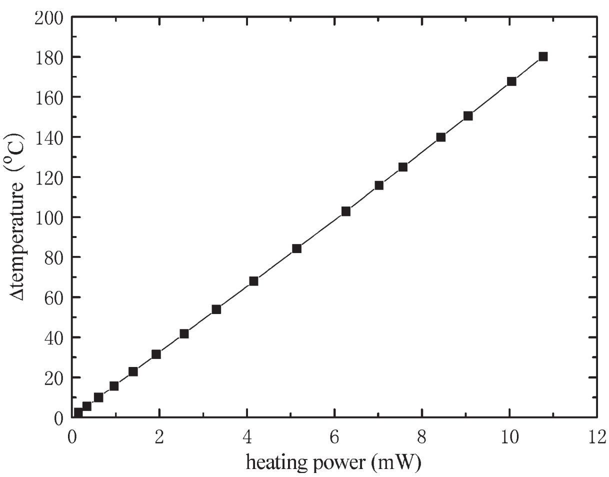

Fig. 7. Thermal impedance (slope) of the tungsten microhotplate.

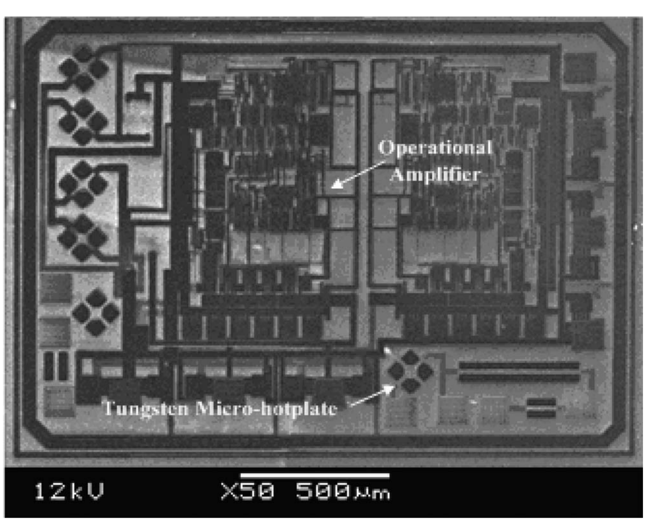

Fig. 8. SEM photograph of the MicroPirani sensor.

the output of the constant-current circuit can provide a wide measurement range.

The monolithic operational amplifier is designed and configured in a constant-current circuit. Fig. 8 shows a SEM photograph of the MicroPirani sensor, including the tungsten microhotplate and the operational amplifier.

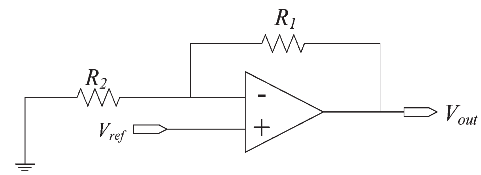

Fig. 9. Constant-current circuit for the sensor.

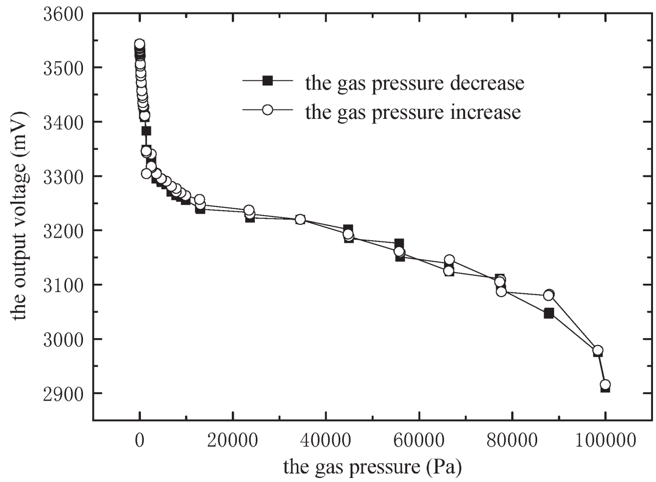

Fig. 10. Measurement results of the MicroPirani pressure sensor based on the tungsten microhotplate, with the gas pressure ranging from 1 to 10^5 Pa.

Fig. 9 is the schematic of the constant-current circuit. R_1 is the tungsten resistor in the microhotplate, and R_2 is the external reference resistor. $V_{\rm ref}$ is the external reference voltage. $V_{\rm out}$ is the output voltage, as shown in

$$V_{\rm out} = V_{\rm ref}\left(1 + \frac{R_1}{R_2}\right). \tag{6}$$

The output of the amplifier reflects the resistance variation of R_1. The resistance of R_1 increases as the gas pressure decreases. Thus, the output voltage increases as the gas pressure decreases.

The value of R_1 is 230 Ω, and $V_{\rm ref}$ is 1.25 V in the measurement. By adjusting R_2, we can obtain the proper current which not only ensures a good performance of the pressure sensor but also avoids the microhotplate in the low gas pressure to be destroyed. The bias current is 7 mA in the measurement. The vacuum system used for the measurements is available in the pressure range from 0.1 Pa to atmosphere. The sensor is fixed in the cylindrical chamber, and the measurement procedure is divided into two steps. First, the gas pressure is decreased from atmosphere to 0.1 Pa. Second, when the gas pressure of the vacuum system is below 1 Pa, the pump is isolated, the gas slowly bleeds into the chamber to the desired pressure, and then, the real-time output voltage of the circuit is recorded with a personal computer using an A/D card. The results are shown in Figs. 10 and 11. In Fig. 10, as the gas pressure changes from 1 to 10^5 Pa, the output voltage changes from 2900 to 3543 mV, which can be easily measured. In the low gas pressure from 1 to 100 Pa, in Fig. 11, the full range of output voltage is from 3520

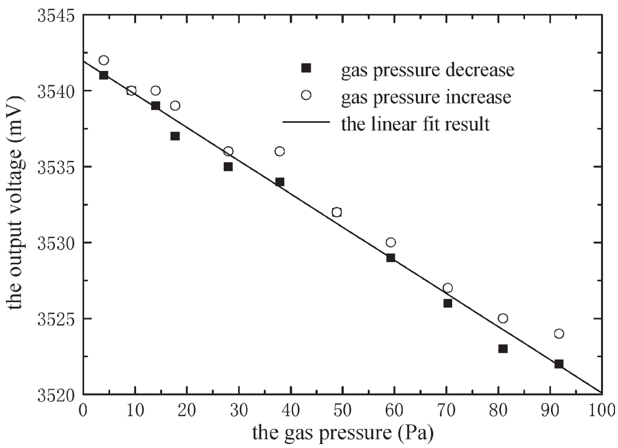

Fig. 11. Measurement results of the MicroPirani pressure sensor based on the tungsten microhotplate, with the gas pressure ranging from 1 to 100 Pa.

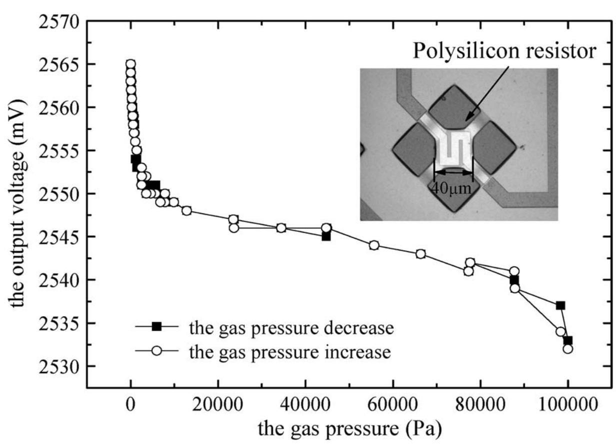

Fig. 12. Measurement results of the MicroPirani pressure sensor based on the polysilicon microhotplate, with the gas pressure ranging from 1 to 10^5 Pa.

to 3543 mV, the sensitivity of the sensor is 0.23 mV/Pa, the linearity is 4.95%, and the hysteresis is 8.69%. The designed MicroPirani pressure sensor can be applied to the medium-vacuum measurement.

In addition, the polysilicon microhotplate is fabricated to measure the gas pressure with the constant-current circuit, as shown in the Fig. 12. In the aforementioned CMOS process, Poly2 is the heating resistor, and Poly1 is employed as the sacrificial layer. The resistance of the heating resistor is 550 Ω, and the temperature coefficient of Poly2 is $1.6 \times 10^{-4}/^{\circ}\mathrm{C}$. The constant current is 2.2 mA in the measurement. The measurement results are shown in Fig. 12. As the gas pressure changes from 1 to 10^5 Pa, the output voltage changes from 2530 to 2565 mV, which is much less than the output-voltage range of the sensor based on the tungsten microhotplate. The reasons for this phenomenon lie in two parts. First, the heating current through the polysilicon resistor is much lower than that in the tungsten resistor because the polysilicon would be destroyed by the high heating current due to its lower melting point (about 1400 $^{\circ}$C) than the tungsten's (about 3400 $^{\circ}$C). Second, in the standard CMOS process, the temperature coefficient of polysilicon is much smaller than that of tungsten. For example, in our CMOS process, the temperature coefficient of polysilicon is $1.6 \times 10^{-4}/^{\circ}\mathrm{C}$, while that of tungsten is $1.5 \times 10^{-3}/^{\circ}\mathrm{C}$.

V. Conclusion

This paper has presented the tungsten microhotplate in a standard CMOS process which has more advantages than the polysilicon microhotplate. Tungsten has many good characteristics, such as high melting point and large temperature coefficient. Tungsten has been traditionally used as a plug material to form via pathways between different metal layers and the silicon substrate in standard integrated circuits. In our design of the tungsten microhotplate, tungsten is employed as the heater in the form of serpentine resistor instead of via plug. The anchors of the tungsten resistor are connected to one metal layer. The measurement results show that the sheet resistance of tungsten changes with different dimensions, and its temperature coefficient is $1.5 \times 10^{-3}/^{\circ}\mathrm{C}$. The thermal impedance of the designed tungsten microhotplate is 17 $^{\circ}\mathrm{C/mW}$.

A MicroPirani pressure sensor is implemented with a tungsten microhotplate. A monolithic constant-current circuit including an operational amplifier is used to bias the tungsten microhotplate to measure the gas pressure. The measurement results show that the tungsten microhotplate has a good response to the gas pressure, particularly in the low gas pressure ranging from 1 to 100 Pa, the sensitivity of the sensor is 0.23 mV/Pa, the linearity is 4.95%, and the hysteresis is 8.69%. The MicroPirani pressure sensor in our study can be applied to the medium-vacuum measurement.

Because tungsten in a standard CMOS process has a large temperature coefficient, a new series of thermal-based sensor products compatible with the standard CMOS process can be developed.

References

[1] B. Borovic, A. Q. Liu, D. Popa, H. Cai, and F. L. Lewis, "Light-intensity-feedback-waveform generator based on MEMS variable optical attenuator," *IEEE Trans. Ind. Electron.*, vol. 55, no. 1, pp. 417–426, Jan. 2008.

[2] M. R. Werner and W. R. Fahrner, "Review on materials, microsensors, systems and devices for high-temperature and harsh-environment applications," *IEEE Trans. Ind. Electron.*, vol. 48, no. 2, pp. 249–257, Apr. 2001.

[3] P. K. Weng and J. S. Shie, "Micro-Pirani vacuum gauge," *Rev. Sci. Instrum.*, vol. 65, no. 2, pp. 492–499, Feb. 1994.

[4] A. W. van Herwaarden and P. M. Sarro, "Double-beam integrated thermal vacuum sensor," *J. Vac. Sci. Technol. A, Vac. Surf. Films*, vol. 5, no. 4, pp. 2454–2457, Jun./Aug. 1987.

[5] J. S. Shie, B. C. S. Chou, and Y. M. Chen, "High performance Pirani vacuum gauge," *J. Vac. Sci. Technol. A, Vac. Surf. Films*, vol. 13, no. 6, pp. 2972–2979, Nov./Dec. 1995.

[6] M. Doms, A. Bekesch, and J. Mueller, "A microfabricated Pirani pressure sensor operating near atmospheric pressure," *J. Micromech. Microeng.*, vol. 15, no. 8, pp. 1504–1510, Aug. 2005.

[7] J. Mitchell, G. R. Lahiji, and K. Najafi, "An improved performance poly Si Pirani vacuum gauge using heat distributing structural supports," in *Proc. IEEE Int. Conf. MEMS*, 2005, pp. 291–294.

[8] M. Doms and J. Mueller, "A micromachined vapor jet pump," *Sens. Actuators A, Phys.*, vol. 119, no. 2, pp. 462–467, Apr. 2005.

[9] J. Chae, J. M. Giachino, and K. Najafi, "Fabrication and characterization of a wafer-level MEMS vacuum package with vertical feedthroughs," *J. Microelectromech. Syst.*, vol. 17, no. 1, pp. 193–200, Feb. 2008.

[10] F. T. Zhang, Z. Tang, J. Yu, and R. C. Jin, "A micro-Pirani vacuum gauge based on micro-hotplate technology," *Sens. Actuators A, Phys.*, vol. 126, no. 2, pp. 300–305, Feb. 2006.

[11] C. H. Mastrangelo and R. S. Muller, "Microfabricated thermal absolute-pressure sensor with on-chip digital front-end processor," *IEEE J. Solid-State Circuits*, vol. 26, no. 12, pp. 1998–2007, Dec. 1991.

[12] H. Baltes, O. Paul, and O. Brand, "Micromachined thermally-based CMOS microsensors," *Proc. IEEE*, vol. 86, no. 8, pp. 1660–1678, Aug. 1998.
[13] O. Paul and H. Baltes, "Novel fully CMOS-compatible vacuum sensor," *Sens. Actuators A, Phys.*, vol. 46/47, no. 1–3, pp. 143–146, Jan./Feb. 1995.
[14] F. Völklein and A. Meier, "Microstructured vacuum gauges and their future perspectives," *Vacuum*, vol. 82, no. 4, pp. 420–430, Dec. 2007.
[15] R. Puers, S. Reyntjens, and D. De Bruyker, "The NanoPirani—An extremely miniaturized pressure sensor fabricated by focused ion beam rapid prototyping," *Sens. Actuators A, Phys.*, vol. 97/98, no. 1, pp. 208–214, Apr. 2002.
[16] C. H. Mastrangelo, "Thermal applications of microbridges," Ph.D. dissertation, Dept. Elect. Eng. Comp. Sci., Univ. California, Berkeley, CA, 1991.
[17] J. Chae, B. H. Stark, and K. Najafi, "A micromachined Pirani gauge with dual heat sinks," *IEEE Trans. Adv. Packag.*, vol. 28, no. 4, pp. 619–625, Nov. 2005.
[18] E. H. Klaassen, "Micromachined instrumentation systems," Ph.D. dissertation, Stanford Univ., Stanford, CA, 1996.
[19] M. Quirk and J. Serda, *Semiconductor Manufacturing Technology*. Englewood Cliffs, NJ: Prentice–Hall, 2001, pp. 299–313.
[20] A. Frazier, R. Warrington, and C. Friedrich, "The miniaturization technologies: Past, present, and future," *IEEE Trans. Ind. Electron.*, vol. 42, no. 5, pp. 423–430, Oct. 1995.
[21] G. Yan, P. Chan, M. Hsing, R. Sharma, J. Sin, and Y. Wang, "An improved TMAH Si-etching solution without attacking exposed aluminum," *Sens. Actuators A, Phys.*, vol. 89, no. 1/2, pp. 135–141, Mar. 2001.

Jiaqi Wang was born in Dalian, China, in 1981. He received the B.S. and M.S. degrees in electronics engineering from Shenyang University of Technology, Shenyang, China, in 2003 and 2006, respectively. He is currently working toward the Ph.D. degree in the Department of Electronic Engineering, Dalian University of Technology, Dalian.

His research interests include micromachining technology, system-on-a-chip, and microscale heat transfer in semiconductor devices.

Zhenan Tang (M'07) was born in Dalian, China, in 1955. He received the B.S. degree in technology physics from Xi'an University of Electronic Science and Technology, Xi'an, China, in 1982, and the M.S. degree in electronic engineering and the Ph.D. degree in mechanical engineering from Dalian University of Technology, Dalian, in 1990 and 1999, respectively.

He is currently a Professor with and the Director of the Microelectronic Institute, Dalian University of Technology. His current research interests include ICs, microelectromechanical systems, and microscale heat transfer in semiconductor devices.

Jinfeng Li was born in Liaoning, China, in 1979. She received the B.S. and M.S. degrees in electronic engineering from Shenyang Institute of Chemical Technology, Shenyang, China, in 2001 and 2004, respectively. She is currently working toward the Ph.D. degree in the Department of Electronic Engineering, Dalian University of Technology, Dalian, China.

Her current research interests include design and test of integrated circuits.

Fengtian Zhang was born in 1976. He received the B.S. and M.S. degrees in engineering from Southwest Petroleum University, Chengdu, China, in 1999 and 2002, respectively, and the D.Eng. degree from Dalian University of Technology, Dalian, China, in 2007.

Since 2007, he has been a Research Associate with the China Academy of Engineering Physics, Mianyang, China, where he is engaged in research and development on microsensors and related conditioning circuits.